

M&MoCS



Shahid Chamran
University of Ahvaz

Journal of Applied and Computational Mechanics



Research Paper

Thermal Buckling Analysis of Functionally Graded Euler-Bernoulli Beams with Temperature-dependent Properties

Wei-Ren Chen¹, Chun-Sheng Chen², Heng Chang³

¹ Department of Mechanical Engineering, Chinese Culture University
Taipei 11114, Taiwan, Email: wrchen@faculty.pccu.edu.tw

² Department of Mechanical Engineering, Lunghwa University of Science and Technology
Guishan Shiang 33306, Taiwan, Email: cschen@mail.lhu.edu.tw

³ Department of Mechanical Engineering, Chinese Culture University
Taipei 11114, Taiwan, Email: hchang@faculty.pccu.edu.tw

Received July 26 2019; Revised August 30 2019; Accepted for publication September 13 2019.

Corresponding author: Wei-Ren Chen (wrchen@faculty.pccu.edu.tw)

© 2020 Published by Shahid Chamran University of Ahvaz

& International Research Center for Mathematics & Mechanics of Complex Systems (M&MoCS)

Abstract. Thermal buckling behavior of functionally graded Euler-Bernoulli beams in thermal conditions is investigated analytically. The beam with material and thermal properties dependent on the temperature and position is considered. Based on the transformed-section method, the functionally graded beam is considered as an equivalent homogeneous Euler-Bernoulli beam with an effective bending rigidity under an eccentric thermal load. Then, the thermal elastic buckling equation associated with the bending deflection about the neutral axis is established. The easily usable closed-form solutions for the critical thermal buckling temperature of functionally graded beams under uniform and non-linear temperature rise are obtained and used to calculate the thermal buckling temperature. Some results are evaluated and compared with those by other investigators to validate the accuracy of the presented method. The effects of material compositions, temperature-dependent material properties, slenderness ratios and restraint conditions on thermal buckling behaviors are discussed. It is believed that the proposed model provides engineers and designers an easy and useful method to investigate the effects of various parameters affecting the thermal buckling characteristics of functionally graded beams.

Keywords: Thermal buckling, Euler-Bernoulli beam, Transformed-section method, Functionally graded beam, Buckling temperature.

1. Introduction

Functionally graded materials (FGMs) are advanced composite materials having material properties varying smoothly in the specified direction by a gradually change in the volume fraction of the constituents. They are usually consisted of the ceramic and metal with the combination of the high toughness of metal and excellent heat resistance of ceramic. Because of the advantages of this combination, FGMs made of metals and ceramics have been largely utilized in several engineering structures in thermal environments. While FGM structures are exposed in high-temperature conditions, they may encounter the thermal buckling problem due to the thermal loading effects. Therefore, to better understand the thermal buckling of FGM structures in thermal conditions is needed from the structural design point of view. For the past decades, the buckling problems [1-13] of FG beams subjected to the mechanical loads had been studied by many researchers. The goal of the present paper is focused on the thermal buckling behaviors of FG beams so only the literature related to the current work is discussed next.

Kiani and Eslami [14] investigated the thermal buckling of FG Euler-Bernoulli beams subjected to different thermal



loadings, by assuming that the material properties vary with a power-law function in the thickness direction. The beam is assumed to be subjected to uniform, linear and nonlinear temperature rises along the thickness direction. Close-form expressions of the critical thermal buckling temperature for FG beams with various end supports were obtained and used to investigate the buckling of bifurcation type. Based on the third-order shear deformation theory, Wattanasakulpong et al. [15] used Ritz method to study the vibration and thermal buckling of FG beams under uniform temperature rise. The influences of material constituents, power law indices, slenderness ratios, temperature-dependent properties and restraint conditions on the natural frequency and thermal buckling temperature were investigated. The results reveal that temperature-dependent properties significantly affect the beams with small slenderness ratio. Kiani et al. [16-17] studied the thermal buckling behavior of piezoelectric FG Euler-Bernoulli and Timoshenko beams, respectively, under various thermal loadings and actuator voltages. The material properties are assumed to change in the thickness following the power-law distribution. Analytical solutions for the critical buckling temperature were formulated and used to examine the effects of the volume fraction index, applied voltage, geometric aspect and restraint types on the bifurcation-type thermal buckling. Fallah and Aghdam [18] dealt with the thermo-mechanical non-linear vibration and buckling of FG Euler-Bernoulli beams resting on non-linear elastic foundations using the Galerkin's decomposition method. The material properties are assumed to change along the thickness direction by a simple power law. Closed-form expressions for the nonlinear natural frequency and critical buckling temperature were derived. The effects of foundation parameters, volume fraction indices, thermal loads, vibration amplitudes and boundary conditions were studied. Fu et al. [19] studied the thermal buckling problem of FG Timoshenko beams with axial crack under uniform temperature rise. The materials properties vary in the thickness direction described by a power law. The buckling equations were established based on the Hamilton's principle and solved using the differential quadrature method to determine the thermal buckling temperature and modes. The effects of volume fraction index, crack size and position on the thermal buckling behavior of the FG beam were presented. Anand Rao et al. [20] analyzed the vibration and thermal buckling of FG Timoshenko beams under uniform temperature rise using the finite element approach. The temperature dependent material properties were considered in the calculations of natural frequencies and critical thermal buckling temperatures. The results indicate that temperature dependence of material properties has a significant impact on the performance of the beam. Based on the virtual displacements principle, Kiani and Eslami [21] investigated the thermal-mechanical buckling behavior of temperature-dependent FG Timoshenko beams. The mechanical and thermal properties are assumed to depend on temperature and the thickness coordinate, and change along the thickness by a power-law distribution. Close-form solutions were determined and used to obtain the critical thermal buckling temperatures of FG beams under uniform, linear and nonlinear temperature distributions, respectively. Esfahani et al. [22] applied the generalized differential quadrature method to investigate the thermal buckling and post-buckling behaviors of temperature-dependent FG Timoshenko beams subjected to uniform and nonlinear temperature changes. The beam is supported on the nonlinear elastic foundation. The influences of the power-law indices, foundation coefficients, thermal loading types, temperature-dependent properties and restrained supports on thermal stability behaviors were discussed.

Ghiasian et al. [23] dealt with the nonlinear thermal dynamic buckling of temperature-dependent FG Timoshenko beams resting on an elastic foundation. Based on the Newton-Raphson method, a set of nonlinear algebraic equations was analyzed to investigate the effects of the geometric imperfection and foundation stiffness on the dynamic buckling of the FG beam under a sudden uniform temperature rise. Based on the shooting method, Sun et al. [24] studied the thermal buckling and post-buckling of FG Timoshenko beams with material properties changing with the power law function in the thickness direction. The beam is supported on nonlinear elastic foundations and subjected to uniform and non-linear temperature rises, respectively. The effects of the slenderness ratio, foundation stiffness and power law exponent on the critical buckling temperature and post-buckling deformations of FG beams were examined. Trinh et al. [25] studied the vibration and buckling behaviors of higher-order shear deformable FG beams under mechanical and thermal loadings using the Hamilton's principle and state space method. The material properties are function of position and temperature, and change along the thickness with the power-law function. Three types of thermal loads, which are uniform temperature rise, linear and nonlinear temperature distributions along the thickness, were considered. The effects of material compositions, volume fraction indices, temperature distributions, slenderness ratios and restraint types on the natural frequencies, critical buckling temperature and buckling loads were investigated. Shen et al. [26] analyzed the thermal buckling of third-order shear deformable twisted FG beams with temperature-dependent material properties based on the Chebyshev-Ritz method. The temperature field is assumed to be uniform or change across the beam thickness. The effects of twist angle, aspect ratios, volume fraction index, temperature-dependent properties and boundary conditions on the thermal buckling behavior of the FG beams were discussed. Nguyen et al. [27] studied the free vibration and buckling of FG beams under various hygro-thermal loadings using the higher-order shear deformation theory. They applied Lagrange's equations to establish the governing equations and used Ritz method to solve the equations. The effects of material, geometric and hygro-thermal parameters on the temperature-independent and temperature-dependent results were presented. Hosseini et al. [28] presented the thermal buckling of FG Timoshenko beams with elastic end supports using Fourier series expansion. The symmetrical and unsymmetrical FG beams subjected to uniform temperature rise were considered. The effects of the material distribution, power law exponent, support stiffness and slenderness ratio on the critical buckling temperature were investigated. Majumdar and Das [29] presented the thermal buckling stability of clamped-clamped FG Euler-Bernoulli beams under linear and nonlinear temperature gradients based on the variational principle and Ritz method. The temperature-dependent material properties are assumed to vary across the thickness with a power-law function. The effects of thermal loading types, volume fraction indices and slenderness ratios on the thermal

buckling loads of various FG beams were examined. Based on the physical neutral plane, Liu et al. [30] investigated the thermal buckling behavior of porous FG sandwich beams using a high-order sinusoidal shear deformation theory. The beams were assumed to be subjected to uniform, linear and nonlinear temperature rises. The influences of porosity, the face-to-core ratio, physical neutral plane, temperature-dependent properties and volume fraction index were discussed. Tran et al. [31] used the isogeometric analysis to investigate the thermal buckling and post-buckling of porous FG microplates with even, uneven and logarithmic-uneven distributions of porosities. The effects of porosity, porosity distribution type, temperature gradient, material gradient index, boundary condition and size-dependent parameter were studied. Zhang et al. [32] studied the elastoplastic thermal buckling behavior of FG beams under non-uniform temperature rise using the symplectic method. The effects of the thermal loading, volume fraction index, aspect ratio, and elastoplastic material parameters on thermal buckling characteristics of the beams were examined.

In most of previous studies, the equations governing the thermal buckling stability of FG beams were formulated by considering the coupling of axial and transverse deformations. Then, various approximate methods were used to reduce the system equations to a set of algebraic eigenvalue equations, which was then solved numerically to obtain the critical thermal buckling temperature. As to the best of the authors' knowledge, no attempt has been made to solve the thermal buckling problem based on the transformed-section method [33]. Hence, the transformed-section method [34-35] is used to study the thermal buckling of FG Euler-Bernoulli beams with material and thermal properties dependent on temperature and the thickness coordinate. The variation of the properties in the thickness direction is described by the power-law function. First, the investigated FG beam is transformed to an equivalent homogeneous Euler-Bernoulli beam with an effective bending rigidity subjected to an eccentric thermal load. Then, the thermal elastic buckling equation of such an equivalent Euler-Bernoulli beam is derived and used to analytically study the thermal buckling of the corresponding FG beam. Because the presented thermal buckling equation is decoupled with the axial mode, only the bending deflection equation is needed to analyze the thermal buckling of the FG beam. Unlike those in the published literature, no algebraic eigenvalue equations are formed and solved in the present study. Instead, the easily usable closed-form expressions for the critical thermal buckling temperature of clamped-clamped and clamped-roller FG beams under uniform and nonlinear temperature rises are obtained and used to evaluate the thermal buckling temperature. Numerous results for the critical thermal buckling temperatures of FG beams with various power law indices, thermal loadings and boundary restraints are calculated and compared with those obtained by other investigators to assure the accuracy of the proposed method. Parametric study is conducted to investigate the effects of the material constituents, material graded indices, temperature-dependent material properties, slenderness ratios and end support conditions on the thermal buckling behaviors of FG beams. It is believed that the present model can facilitate the engineers a simple and effective method to study the thermal buckling behavior of the FG beams.

2. Governing Equations

A functionally graded beam of length L , width b and thickness h is considered. The beam configuration and coordinate systems xyz and $x_1y_1z_1$ are illustrated in Fig. 1. The axis x of coordinate xyz is on the physical midplane xy and its z axis lies in the thickness direction. The x_1 axis of coordinate $x_1y_1z_1$ denotes the neutral axis of the transformed cross-section; the y_1 axis parallels with y axis; the z_1 and z axes coincide with each other. The material and thermal properties of the FG beam are assumed to vary smoothly across the beam thickness with the power-law function.

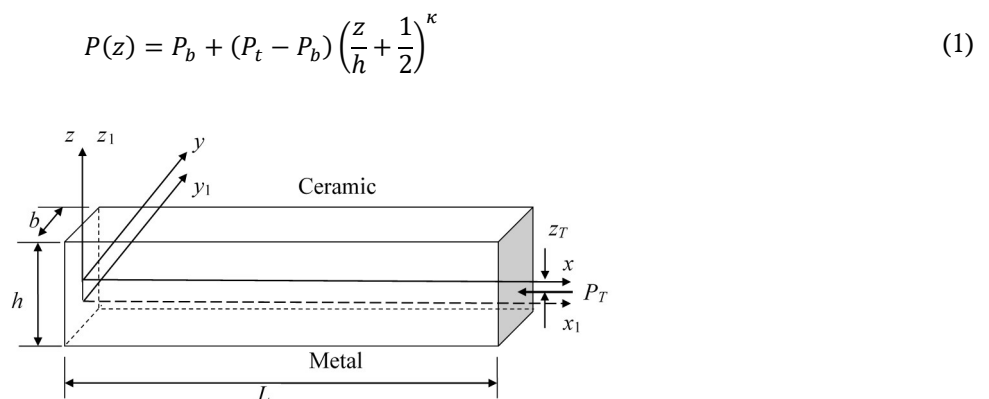


Fig. 1 Beam configuration and coordinate systems.

Here P_t and P_b denote the properties of the top and bottom surfaces of the beam, respectively; κ is the non-negative power-law exponent; z is the thickness coordinate, $-h/2 \leq z \leq h/2$. According to eq. (1), the effective Young's modulus E , thermal expansion coefficient α and thermal conductivity K can be written as follows

$$E(z) = E_b + (E_t - E_b) \left(\frac{z}{h} + \frac{1}{2} \right)^\kappa \quad (2a)$$

$$\alpha(z) = \alpha_b + (\alpha_t - \alpha_b) \left(\frac{z}{h} + \frac{1}{2} \right)^\kappa \quad (2b)$$

$$K(z) = K_b + (K_t - K_b) \left(\frac{z}{h} + \frac{1}{2} \right)^\kappa \quad (2c)$$

in which the subscripts t and b denote the materials at the top and bottom surfaces, respectively. When the temperature dependence of material properties is considered, the nonlinear equation of the Touloukian model [36] is used to evaluate the thermal-elastic material properties as follows

$$P = P_0(P_{-1}T^{-1} + 1 + P_1T + P_2T^2 + P_3T^3) \quad (3)$$

where P_0, P_{-1}, P_1, P_2 and P_3 are coefficients associated with the constituent; $T = T_0 + \Delta T$ in which T_0 and ΔT is the ambient temperature (300 K) and temperature difference.

Considering the FG beam whose temperature is increased from the reference temperature T_0 to the current temperature T , it can be regarded as a beam subjected to a thermal compressive load P_T at a distance z_T as shown in Fig. 1. They are obtained as follows

$$P_T = - \int E(z) \alpha(z) (T - T_0) dA \quad (4)$$

$$z_T = \frac{\int E(z) \alpha(z) z (T - T_0) dA}{\int E(z) \alpha(z) (T - T_0) dA} \quad (5)$$

To derive the differential equations governing the bending deflection of the above FG beam under a thermal compressive load using the transformed-section method, the original rectangular cross section (Fig. 2a) of functionally graded material with two compositions is transformed to an equivalent cross-section of the material at the top surface (Fig. 2b). A modular ratio, $n(z)$, is defined as

$$n(z) = \frac{E(z)}{E_t} = \bar{E} + (1 - \bar{E}) \left(\frac{z}{h} + \frac{1}{2} \right)^\kappa \quad (6)$$

where $\bar{E} = E_b/E_t$. Then, the centroid h_0 and the effective second area moment I_e about the neutral axis of this equivalent cross-section can be obtained as follows

$$h_0 = \frac{\int_{A_t} z dA}{\int_{A_t} dA} = \frac{\kappa(1 - \bar{E})}{2(\kappa + 2)(1 + \kappa\bar{E})} h \quad (7)$$

$$I_e = \int_{A_t} z_1^2 dA = \frac{bh^3}{12} \left[\bar{E} + 12(1 - \bar{E}) \left(\frac{1}{\kappa + 3} - \frac{1}{\kappa + 2} + \frac{1}{4\kappa + 4} \right) - \frac{3\kappa^2(1 - \bar{E})}{(\kappa + 1)(\kappa + 2)^2(1 + \kappa\bar{E})} \right] \quad (8)$$

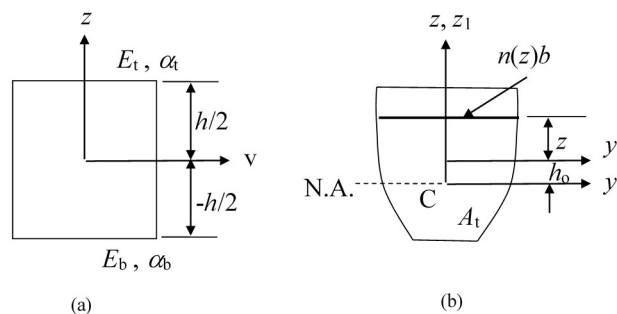


Fig. 2 Beam of functionally graded materials: (a) Original section; (b) Transformed section.

The detailed derivations of above expressions can be referred to the authors' previous work [34]. Hence, the equivalent beam with the transformed cross-section is then considered as a homogeneous beam with an effective bending rigidity $E_t I_e$ and subjected to an eccentric thermal load P_T at a distance $e = h_0 - z_T$ from the centroidal axis of the beam.

By applying the bending deflection equation associated with homogeneous uniform Euler-Bernoulli beams under an eccentric load to the FG beam with the transformed section composed of only material at the top surface, we can yield the following governing equation for the deflection of the FG beam under the thermal compressive load P_T at the end supports

$$\frac{d^4 w}{dx_1^4} + \beta^2 \frac{d^2 w}{dx_1^2} = 0 \quad (9a)$$

where

$$\beta^2 = \frac{P_T}{E_t I_e} \quad (9b)$$

Here w is the bending displacement along the z_1 direction about the neutral axis x_1 . To investigate the thermal buckling behaviors of bifurcation type [21], only the FG beams with the clamped-clamped (CC) and clamped-roller (CR) end supports are considered. For the present boundary conditions, they can be given as

$$\text{Clamped: } w = 0, w' = 0 \quad (10a)$$

$$\text{Roller: } w' = 0, w''' = 0 \quad (10b)$$

In the following, the solutions of the thermal buckling temperature for the uniform equivalent beam with CC and CR boundary conditions will be obtained by using eqs. (9) and (10).

3. Thermal Buckling Analysis

The general solution of the thermal buckling problem for the FG beam in eq. (9) is

$$w(x_1) = C_1 \cos \beta x_1 + C_2 \sin \beta x_1 + C_3 + C_4 x_1 \quad (11)$$

which represents the buckling mode of the beam. The values of C_1 , C_2 , C_3 , C_4 and β can be obtained by properly imposing the boundary conditions in eq. (11). For clamped-clamped FG beams, introducing the conditions $w(0) = w(L) = 0$ and $w'(0) = w'(L) = 0$ into eq. (11) yields the following eigenvalue equation

$$\begin{bmatrix} 1 & 0 & 1 & 0 \\ \cos \beta L & \sin \beta L & 1 & L \\ 0 & \beta & 0 & 1 \\ -\beta \sin \beta L & \beta \cos \beta L & 0 & 1 \end{bmatrix} \begin{Bmatrix} C_1 \\ C_2 \\ C_3 \\ C_4 \end{Bmatrix} = 0 \quad (12)$$

The condition for a nontrivial solution of eq. (12) is that its determinant of the coefficient matrix has to be null, which leads to

$$\sin \frac{\beta L}{2} \left(2\beta L \cos \frac{\beta L}{2} - 4 \sin \frac{\beta L}{2} \right) = 0 \quad (13)$$

Hence, the smallest critical value $\beta_{cr} L$ satisfying eq. (13) is 2π . The critical thermal buckling load $(P_T)_{cr}$ of the clamped-clamped FG beam can be obtained from eq. (9b) as

$$(P_T)_{cr} = (2\pi)^2 \frac{E_t I_e}{L^2} \quad (14)$$

With the boundary conditions $w(0) = w'(0) = 0$ and $w'(L) = w'''(L) = 0$, the eigenvalue equation for the clamped-roller FG beam can be obtained as

$$\begin{bmatrix} 1 & 0 & 1 & 0 \\ 0 & \beta & 0 & 1 \\ -\beta \sin \beta L & \beta \cos \beta L & 0 & 1 \\ \beta^3 \sin \beta L & -\beta^3 \cos \beta L & 0 & 0 \end{bmatrix} \begin{Bmatrix} C_1 \\ C_2 \\ C_3 \\ C_4 \end{Bmatrix} = 0 \quad (15)$$

Similarly, to obtain the nontrivial solution of eq. (15), the singular coefficient matrix yields

$$\beta^4 \sin \beta L = 0 \quad (16)$$

Thus, the smallest critical value $\beta_{cr} L = \pi$. The critical thermal buckling load $(P_T)_{cr}$ for the clamped-roller FG beam is

$$(P_T)_{cr} = \pi^2 \frac{E_t I_e}{L^2} \quad (17)$$

In the present study, the temperature field is assumed to change merely along the thickness direction of the beam. Two typical thermal conditions, uniform temperature rise and nonlinear temperature change, are investigated. For the FG beams under uniform temperature rise, we have

$$\Delta T = T - T_0 \quad (18)$$

in which T_0 and T represent the initial and final temperature, respectively. Thus, the thermal load is obtained from eq. (4) as

$$P_T = E_t \alpha_t A \Delta T \left[\frac{(1 - \bar{E})(1 - \bar{\alpha})}{2\kappa + 1} + \frac{(1 - \bar{E})\bar{\alpha} + \bar{E}(1 - \bar{\alpha})}{\kappa + 1} + \bar{E}\bar{\alpha} \right] = B E_t \alpha_t A \Delta T \quad (19)$$

where $\bar{\alpha} = \alpha_b/\alpha_t$. Substituting eq. (19) into eqs. (14) and (17), the critical thermal buckling temperature for FG beams with temperature-independent (TID) material properties can be obtained as

$$(\Delta T)_{cr} = \frac{(\beta_{cr}L)^2 I_e}{B\alpha_t AL^2} \quad (20)$$

where $\beta_{cr}L = 2\pi$ and π for the clamped-clamped and clamped-roller FG beams, respectively.

For the FG beams subjected to nonlinear temperature rise, the temperature field $T(z)$ across the thickness is governed by one dimensional steady state heat conduction equation with the prescribed temperature conditions at the top and bottom surface

$$\begin{aligned} \frac{d}{dz} \left(K(z) \frac{dT}{dz} \right) &= 0 \\ T\left(\frac{h}{2}\right) &= T_t, \quad T\left(-\frac{h}{2}\right) = T_b \end{aligned} \quad (21)$$

The temperature field of eq. (21) can be determined by using polynomial series as

$$T(z) = T_b + \frac{R_2}{R_1} \Delta T \quad (22a)$$

with

$$\begin{aligned} R_1 &= \sum_{j=0}^n \frac{(-1)^j}{(j\kappa + 1)} \bar{K}^j \\ R_2 &= \sum_{j=0}^n \frac{(-1)^j}{(j\kappa + 1)} \bar{K}^j \left(\frac{z}{h} + \frac{1}{2} \right)^{j\kappa+1} \end{aligned} \quad (22b)$$

in which $\Delta T = T_t - T_b$ is the temperature difference between the top and bottom surfaces of the FG beam; $\bar{K} = (K_t - K_b)/K_b$. Sufficient terms of the series should be taken in the calculation of the temperature distribution. Introducing eq. (22) into eq. (4) yields the following thermal load

$$\begin{aligned} P_T &= D_1 E_t \alpha_t A (T_b - T_0) + D_2 E_t \alpha_t A \Delta T \\ D_1 &= \frac{(1 - \bar{E})(1 - \bar{\alpha})}{2\kappa + 1} + \frac{(1 - \bar{E})\bar{\alpha} + \bar{E}(1 - \bar{\alpha})}{\kappa + 1} + \bar{E}\bar{\alpha} \\ D_2 &= \frac{1}{R_1} \left\{ \sum_{j=0}^n \frac{(-\bar{K})^j}{(j\kappa + 1)} \left[\frac{(1 - \bar{E})(1 - \bar{\alpha})}{(j+2)\kappa + 2} + \frac{(1 - \bar{E})\bar{\alpha} + \bar{E}(1 - \bar{\alpha})}{(j+1)\kappa + 2} + \frac{\bar{E}\bar{\alpha}}{j\kappa + 2} \right] \right\} \end{aligned} \quad (23)$$

Substituting eq. (23) into eqs. (14) and (17), the temperature-independent critical thermal buckling temperature for clamped-clamped and clamped-roller FG beams under nonlinear temperature change can be determined as

$$\Delta T_{cr} = \frac{(\beta_{cr}L)^2 I_e}{D_2 \alpha_t AL^2} + \frac{D_1 (T_b - T_0)}{D_2} \quad (24)$$

To obtain the thermal buckling temperature for FG beams with temperature-dependent (TD) material properties using eqs. (20) and (24), an iteration procedure [15, 29] is needed. The detailed procedures are given as follows.

- Begin with an initial temperature $T_i = T_0$ or T_b . Then calculate the material properties at $T = T_i$ using eq. (3) and determine the effective second area moment using eq. (8).
- Determine the critical thermal buckling temperature difference $(\Delta T_{cr})_i$ using eq. (20) or eq. (24).
- Let the current temperature $T_{i+1} = T_i + (\Delta T_{cr})_i$. Recalculate the material properties at $T = T_{i+1}$ using eq. (3) and determine the new effective second area moment using eq. (8).
- Determine the new critical thermal buckling temperature difference $(\Delta T_{cr})_{i+1}$ using eq. (20) or eq. (24).
- Evaluate the error $\varepsilon = \left| \frac{(\Delta T_{cr})_{i+1} - (\Delta T_{cr})_i}{(\Delta T_{cr})_i} \right|$ to check the convergence. If $\varepsilon \leq 5 \times 10^{-6}$, then the final solution $\Delta T_{cr} = (\Delta T_{cr})_{i+1}$; otherwise, let $i = i+1$ and repeat steps (iii) to (v).

4. Results and Discussion

The present work studies the thermal buckling behaviors of various ceramic-metal FG beams by varying the material parameters, slenderness ratios, thermal loadings and restraint conditions. Three types of FG beams constructed from $\text{Si}_3\text{N}_4/\text{SUS304}$ (S/S), $\text{ZrO}_2/\text{SUS304}$ (Z/S) and $\text{Al}_2\text{O}_3/\text{SUS304}$ (A/S), respectively, are considered. Table 1 [37-38] presents the temperature-dependent coefficients of various material properties for certain ceramic and metal materials. Each of

these FG beams is assumed to subject to uniform temperature rise (UTR) and nonlinear temperature rise (NTR), respectively. For NTR case, the temperature at the bottom surface of the beam is taken to be a constant value of $T_b = 305\text{K}$.

Table 1. Temperature-dependent coefficients of thermal and material properties for various ceramics and metals.

Material	P_0	P_{-1}	P_1	P_2	P_3
Al₂O₃					
E	349.55e+9	0	-3.853e-4	4.027e-7	-1.673e-10
α	6.8269e-6	0	1.838e-4	0	0
ν	0.26	0	0	0	0
K	-14.087	-1123.6	-6.227-3	0	0
Si₃N₄					
E	348.43e+9	0	-3.070e-4	2.160e-7	-8.946e-11
α	5.8723e-6	0	9.095e-4	0	0
ν	0.24	0	0	0	0
K	13.723	0	-1.032e-3	5.466e-7	-7.876e-11
ZrO₂					
E	244.27e+9	0	-1.371e-3	1.214e-6	-3.681e-10
α	12.766e-6	0	-1.491e-3	1.006e-5	-6.778e-11
ν	0.2882	0	1.133e-4	0	0
K	1.7	0	1.276e-4	6.648e-8	0
SUS304					
E	201.04e+9	0	3.079e-4	-6.534e-7	0
α	12.330e-6	0	8.086e-4	0	0
ν	0.3262	0	-2.002e-4	3.797e-7	0
K	15.379	0	-1.264e-3	2.092e-6	-7.223e-10
Ni					
E	223.95e+9	0	-2.794e-4	-3.998e-9	0
α	9.9209e-6	0	8.705e-4	0	0
ν	0.3100	0	0	0	0

As stated in the previous section, the convergence check is conducted while determining the critical thermal buckling temperature of FG beams with temperature-dependent material properties based on the iteration procedure. Fig. 3 illustrates the convergence of the temperature-dependent critical thermal buckling temperature with respect to the iteration number for various clamped-clamped FG beams with $L/h = 40$ and $\kappa = 0.5$ subjected to nonlinear temperature rise. As observed, the solutions converge as the numbers of iteration are increased. To validate the accuracy of the present work, various analytical results are evaluated and compared with those in the published literature. First, the example to be concerned is the thermal buckling of clamped-clamped ZrO₂/Ni (Z/N) FG beams with $L/h = 50$ under uniform temperature rise.

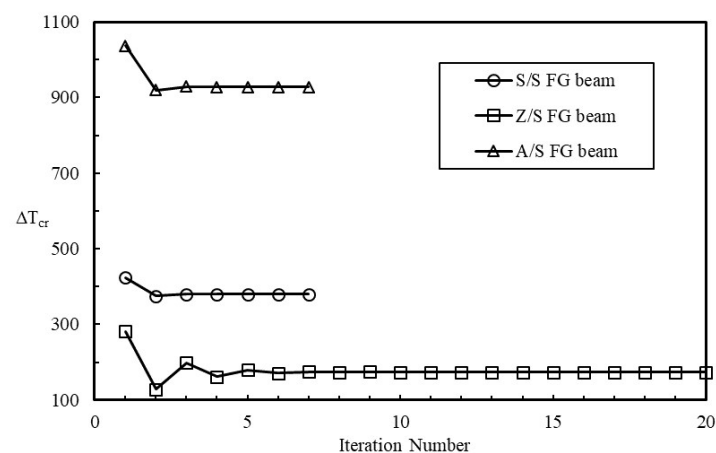


Fig. 3. Critical thermal buckling temperature ΔT_{cr} (K) against iteration number for various clamped-clamped FG beams under NTR ($L/h = 40$, $k = 0.5$).

Table 2 gives the results of the dimensionless critical buckling temperature $\lambda = \Delta T_{cr}(l/h)^2 \alpha_{b0}$ with various values of κ alongside with those by Anand Rao et al. [20], where α_{b0} is the thermal expansion coefficient at $T = 300\text{K}$ of the material at the bottom surface. The present TID and TD solutions match well with the results by Anand Rao et al. [20]. Secondly, the thermal buckling of S/S FG beams with $L/h = 25$ under uniform temperature rise is considered. Table 3 presents the values of TID and TD critical buckling temperature with different values of κ for the FG beams with CC and CR boundary conditions, respectively. The present results agree well with those given by Esfahani et al. [22]. Finally, the thermal buckling of clamped-clamped and clamped-roller S/S FG beams with $L/h = 40$ under nonlinear temperature rise

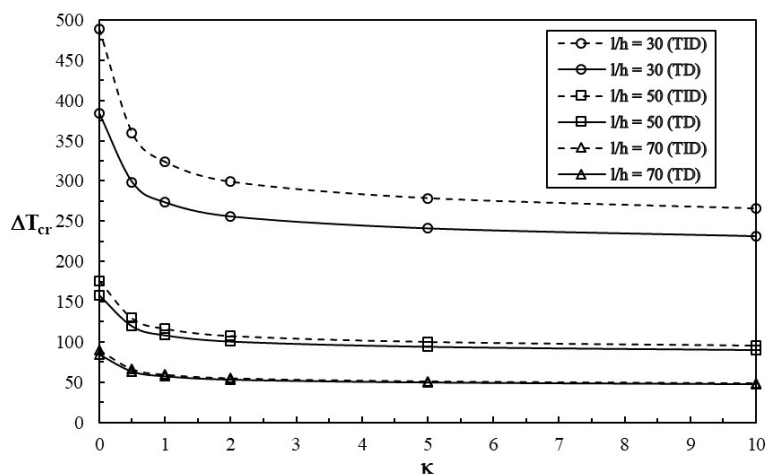
is investigated. Table 4 gives the critical buckling temperature of the S/S FG beams with various values of κ . In comparison with the data obtained by Esfahani et al. [22], the present results also yield good agreement with the published ones. The differences between the compared results in Tables 2-4 are due to the fact that the shear deformation effect is neglected in the present study. As expected, the difference is becoming smaller as the FG beam has a higher value of L/h

Table 2. Comparison of dimensionless critical thermal buckling temperature λ for clamped-clamped Z/N FG beams with $L/h = 50$ under uniform temperature rise.

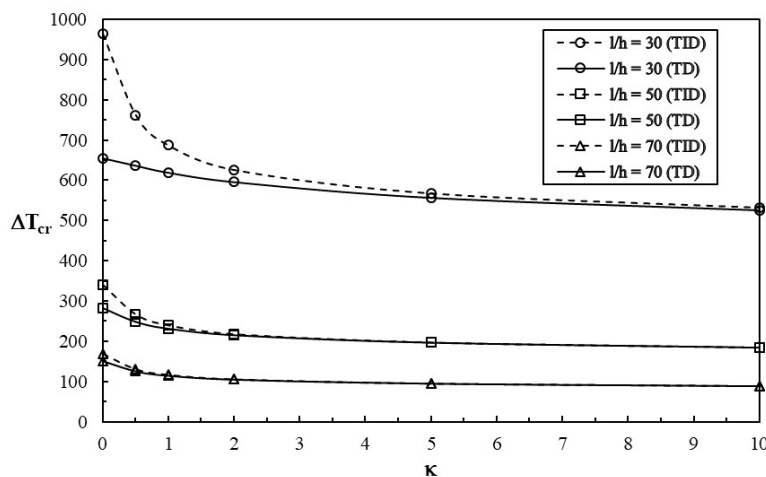
	Source	$\kappa = 0$	0.5	1	10
TID	Present	2.2141	2.5093	2.6553	3.0986
	Anand Rao et al. [20]	2.2056	2.4996	2.6452	3.0870
TD	Present	1.8358	2.1126	2.2653	2.8180
	Anand Rao et al. [20]	1.8299	2.1056	2.2578	2.8084

Table 3. Comparison of critical thermal buckling temperature ΔT_{cr} (K) for S/S FG beams with $L/h = 25$ under uniform temperature rise.

BC	Source	$\kappa = 0$	0.5	1	2	5	10	∞
CR	TID	Present	176.06	129.54	116.55	107.67	100.32	85.89
		Esfahani et al. [22]	175.32	129.02	116.07	107.21	99.88	85.53
	TD	Present	158.18	119.76	108.61	100.87	94.38	81.56
		Esfahani et al. [22]	157.58	119.30	108.16	100.46	93.98	81.24
CC	TID	Present	704.23	518.18	466.20	430.67	401.29	343.57
		Esfahani et al. [22]	692.70	509.89	458.68	423.53	394.39	337.94
	TD	Present	514.84	404.77	372.30	350.07	331.32	289.16
		Esfahani et al. [22]	508.17	399.50	367.32	345.15	326.40	285.06



(a)



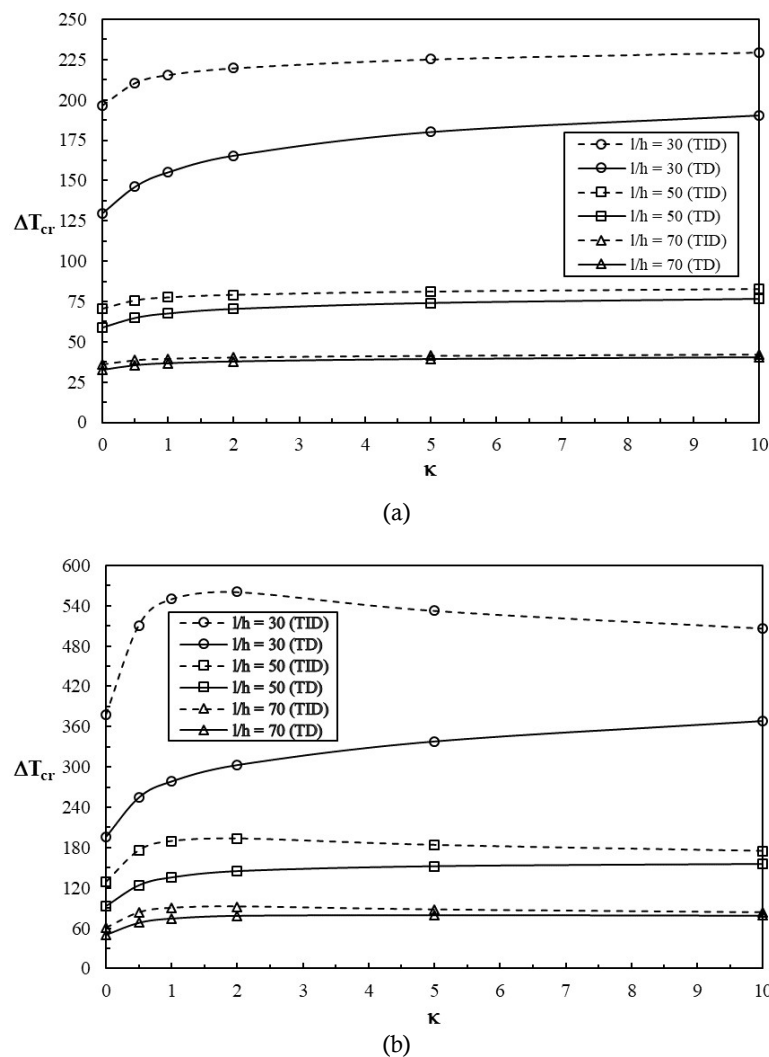
(b)

Fig. 4. Critical thermal buckling temperature ΔT_{cr} (K) of clamped-clamped S/S FG beams with various L/h . (a) UTR (b) NTR.

Table 4. Comparison of critical thermal buckling temperature ΔT_{cr} (K) for S/S FG beams with $L/h = 40$ under nonlinear temperature rise.

BC		Source	$\kappa = 0$	0.5	1	2	5	10	∞
CR	TID	Present	127.06	97.98	87.31	78.86	70.90	66.05	56.89
		Esfahani et al. [22]	127.32	97.97	87.23	78.74	70.77	65.92	56.77
	TD	Present	116.55	94.90	85.92	78.35	70.73	65.94	56.89
		Esfahani et al. [22]	116.74	94.88	85.85	78.23	70.60	65.81	56.77
CC	TID	Present	538.22	424.27	381.66	347.46	314.81	294.92	257.54
		Esfahani et al. [22]	536.62	422.18	379.47	345.22	312.64	292.87	255.81
	TD	Present	413.52	379.73	359.90	339.12	312.22	293.36	257.54
		Esfahani et al. [22]	412.24	377.96	357.94	337.03	310.12	291.35	255.81

In the next, the thermal buckling characteristics of various S/S, Z/S and A/S FG beams with different restraint conditions and thermal loadings are investigated. Figures 4 to 6 show the variations of critical buckling temperature with respect to the power-law exponent κ for the respective clamped-clamped S/S, Z/S and A/S FG beam with different L/h ratios under UTR and NTR thermal gradients. As seen in Fig. 4, both TID and TD solutions for the critical buckling temperatures of the S/S FG beam decrease with the increasing volume fraction index κ . The critical thermal buckling temperature decreases dramatically as κ increases from 0 to 1, but reduces slightly thereafter. However, the discrepancy between the TID and TD solutions decreases significantly when the slenderness ratio and volume fraction index increase, especially for the FG beam under NTR. Unlike the S/S FG beam, both TID and TD solutions in Fig. 5(a) for Z/S FG beams under UTR increases with the increase in κ . In Fig. 5(b), the buckling temperature of TD solution for Z/S FG beams under NTR continuously enlarges with the increasing κ , while that of TID solution increases firstly and reaches a maximum, then decrease thereafter. It is noted that the critical buckling temperature of FG beams with small slenderness ratio is considerably affected by the temperature-dependent material properties. Meanwhile, the influence is diminished as the slenderness ratio and volume fraction index are increased.

**Fig. 5.** Critical thermal buckling temperature ΔT_{cr} (K) of clamped-clamped Z/S FG beams with various L/h . (a) UTR (b) NTR.

Similar to the S/S FG beam, it is seen in Fig. 6(a) that both TID and TD solutions of A/S FG beams under UTR decrease sharply with κ initially and then reduce gradually. The results also show that the effects of temperature-dependent material properties become less significant for A/S beams with higher slenderness ratio and volume fraction index. Unlike the beams under UTR, the values for the critical buckling temperatures of A/S FG beams under NTR increase continuously with κ . However, the critical thermal buckling temperature could not be obtained when κ is increased up to a typical value. As observed in Fig. 6(b), the critical buckling temperature of the A/S FG beam could be obtained up to a higher value of κ as the beam has a higher L/h ratio. As cited by Majumdar and Das [29], it is attributable to the fact that the values of the effective Young's modulus and/or thermal expansion coefficient of FG materials are very lower under high-temperature environments, which is encountered for A/S FG beams under NTR. As expected, the results in Figs. 4 to 6 reveal that the critical buckling temperature decreases with the increasing slenderness ratio.

Figures 7(a) and 7(b) illustrate the results of the critical buckling temperature with the power-law exponent κ for the respective clamped-clamped S/S, Z/S and A/S FG beam with $L/h = 40$ under UTR and NTR, respectively. As observed, the A/S FG beam has the highest buckling temperature, followed by the S/S FG beam and Z/S FG beam irrespective of the thermal loading type. In the case of UTR, the critical buckling temperature of the A/S FG beam is approaching to that of the S/S FG beam when increases κ from 2 to 10. As seen in Fig. 7(b), the A/S FG beam under NTR exhibits an apparently high buckling temperature as κ increases from 0 to 1 compared to the S/S and Z/S beam.

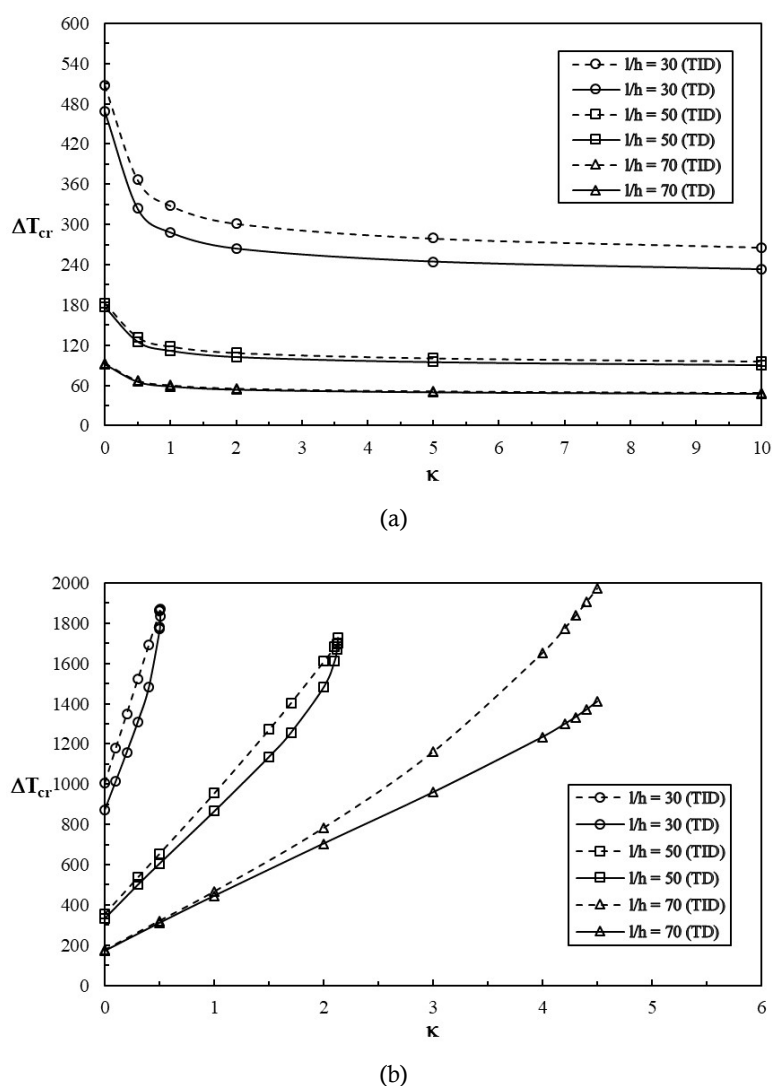


Fig. 6. Critical thermal buckling temperature ΔT_{cr} (K) of clamped-clamped A/S FG beams with various L/h . (a) UTR (b) NTR.

Tables 5 and 6 show the effects of the slenderness ratios and volume fraction indices on the critical buckling temperature of clamped-roller FG beams subjected to UTR and NTR types of thermal loadings. Compared to the corresponding clamped-clamped one, the clamped-roller beam has a smaller buckling temperature because CR end support is softer than the CC end support. Similar behaviors of the variations of critical buckling temperature with κ and L/h for various clamped-clamped FG beams as discussed previously can also be seen for the corresponding clamped-roller ones.

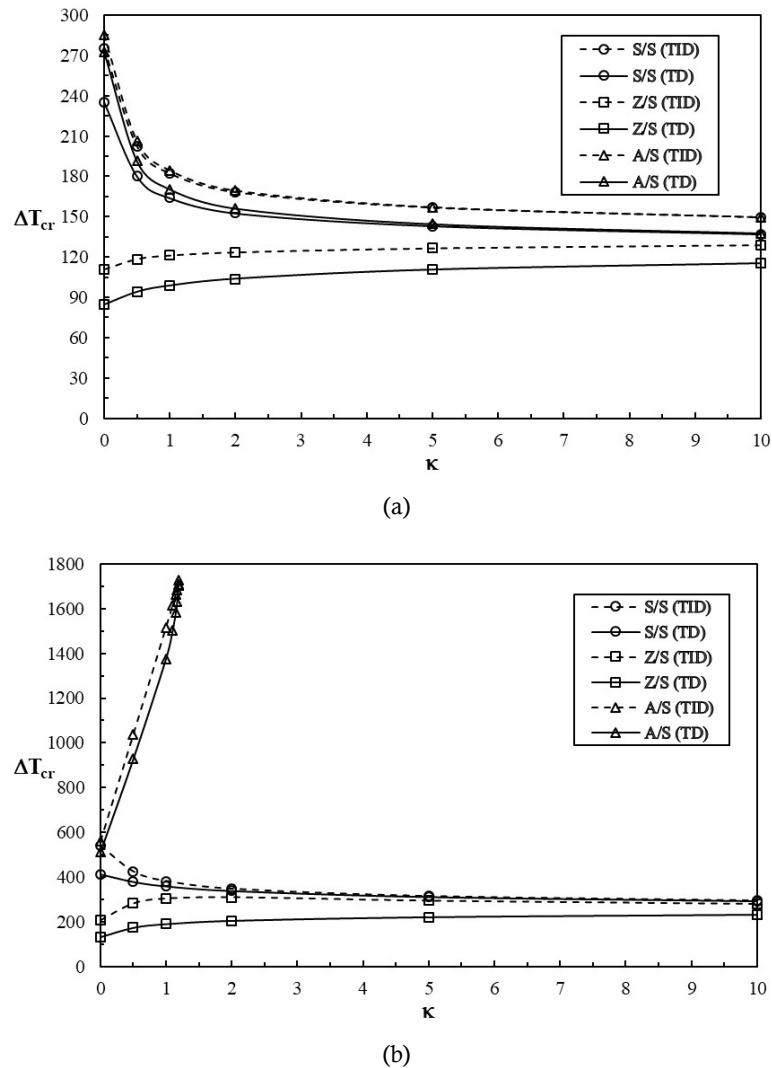


Fig. 7. Critical thermal buckling temperature ΔT_{cr} (K) of various clamped-clamped FG beams with $L/h = 40$. (a) UTR (b) NTR.

Table 5. Critical thermal buckling temperature ΔT_{cr} (K) of various clamped-rolled FG beams with various L/h under uniform temperature rise.

BC	L/h		$\kappa = 0$	0.5	1	2	5	10	∞
S/S	30	TID	122.26	89.96	80.94	74.77	69.67	66.44	59.65
		TD	113.12	85.03	76.95	71.36	66.69	63.73	57.50
	40	TID	68.77	50.60	45.53	42.06	39.19	37.37	33.55
		TD	65.69	48.97	44.21	40.93	38.21	36.48	32.85
	50	TID	44.01	32.39	29.14	26.92	25.08	23.92	21.47
		TD	42.71	31.70	28.59	26.45	24.67	23.55	21.18
Z/S	30	TID	22.46	16.52	14.87	13.73	12.80	12.20	10.96
		TD	22.11	16.34	14.72	13.61	12.69	12.11	10.88
	40	TID	49.16	52.64	53.88	54.93	56.29	57.37	59.65
		TD	42.90	46.99	48.77	50.53	52.78	54.38	57.50
	50	TID	27.65	29.61	30.31	30.90	31.67	32.27	33.55
		TD	25.51	27.72	28.61	29.45	30.51	31.29	32.85
A/S	30	TID	17.70	18.95	19.40	19.78	20.27	20.65	21.47
		TD	16.79	18.15	18.68	19.17	19.79	20.25	21.18
	40	TID	9.03	9.67	9.90	10.09	10.34	10.54	10.96
		TD	8.78	9.46	9.71	9.93	10.21	10.43	10.88
	50	TID	126.87	91.71	82.02	75.36	69.88	66.52	59.65
		TD	124.18	88.52	79.00	72.47	67.12	63.93	57.50
A/S	30	TID	71.36	51.59	46.13	42.39	39.31	37.42	33.55
		TD	70.50	50.55	45.15	41.44	38.40	36.56	32.85
	40	TID	45.67	33.01	29.53	27.13	25.16	23.95	21.47
		TD	45.31	32.58	29.12	26.74	24.78	23.59	21.18
	50	TID	23.30	16.84	15.06	13.84	12.83	12.22	10.96
		TD	23.21	16.73	14.96	13.74	12.73	12.12	10.88

Table 6. Critical thermal buckling temperature ΔT_{cr} (K) of various clamped-rolled FG beams with various L/h under nonlinear temperature rise.

BC	L/h		$\kappa = 0$	0.5	1	2	5	10	∞
S/S	30	TID	233.65	182.57	163.62	148.49	134.13	125.38	108.91
		TD	202.90	172.95	159.23	146.92	133.64	125.07	108.91
	40	TID	127.05	97.98	87.31	78.86	70.90	66.05	56.89
		TD	116.55	94.90	85.92	78.35	70.72	65.94	56.89
	50	TID	77.72	58.83	51.98	46.62	41.63	38.58	32.81
		TD	73.36	57.60	51.43	46.41	41.55	38.53	32.81
	70	TID	34.75	24.73	21.23	18.56	16.14	14.67	11.84
		TD	33.70	24.45	21.10	18.50	16.12	14.66	11.84
	Z/S	TID	86.79	118.29	127.58	130.24	123.98	118.01	108.91
		TD	67.85	91.02	99.50	105.48	108.44	108.79	108.91
		TID	44.45	61.03	65.99	67.50	64.42	61.43	56.89
		TD	38.21	52.06	56.89	59.72	59.80	58.79	56.89
		TID	24.84	34.53	37.49	38.47	36.85	35.23	32.81
		TD	22.45	31.10	34.04	35.58	35.19	34.30	32.81
		TID	7.78	11.46	12.66	13.18	12.84	12.43	11.84
		TD	7.37	10.86	12.07	12.70	12.57	12.28	11.84
A/S	30	TID	243.51	446.63	650.68	1094.66	NA	NA	108.91
		TD	233.61	424.39	606.21	964.01	NA	NA	108.91
	40	TID	132.60	239.94	347.48	581.61	1758.27	NA	56.89
		TD	129.46	234.02	336.21	536.30	1104.81	NA	56.89
	50	TID	81.26	144.27	207.14	344.15	1032.71	NA	32.81
		TD	80.01	142.31	204.41	332.38	683.46	NA	32.81
	70	TID	36.56	60.96	84.94	137.37	400.93	NA	11.84
		TD	36.27	60.61	84.79	139.66	347.43	NA	11.84

5. Conclusions

The thermal buckling analysis for the FG Euler-Bernoulli beam with the power law function of material distribution was established based on the transformed-section method. Analytical solutions of the critical buckling temperature were derived for the clamped-clamped and clamped-roller FG beams under uniform and nonlinear temperature changes. The critical thermal buckling loads for typical examples were analytically evaluated and compared with the published data to verify the accuracy of the presented model. A good agreement between the compared results was achieved. The proposed model was then applied to investigate the influences of the material constituents, material distributions, slenderness ratios, temperature distributions and boundary conditions on the thermal buckling behaviors of various FG beams. The results revealed that these parameters significantly affect the thermal buckling characteristics of FG beams. It is believed that the present analytical solutions give engineers a good insight in the parameters of the FG beam affecting its thermal buckling characteristics. This paper focused on the thermal buckling stability analysis of the temperature-dependent FG beams with simple rectangular cross-section. In the future work, more complex annulus cross-section should be considered in order to demonstrate the general applicability of the proposed method.

Conflict of Interest

The authors declared no potential conflicts of interest with respect to the research, authorship and publication of this article.

Funding

The authors would like to thank the financial support from Chinese Culture University.

References


- [1] Yang, J., Chen, Y., Free vibration and buckling analyses of functionally graded beams with edge cracks, *Composite Structures*, 83, 2008, 48-60.
- [2] Nguyen, T.K., Vo, T.P., Thai, H.T., Static and free vibration of axially loaded functionally graded beams based on the first-order shear deformation theory, *Composites: Part B*, 55, 2013, 147-157.
- [3] Li, S.R., Batra, R.C., Relations between buckling loads of functionally graded Timoshenko and homogeneous Euler-Bernoulli beams, *Composite Structures*, 95, 2013, 5-9.
- [4] Li, S.R., Wang, X., Wan, Z., Classical and homogenized expressions for buckling solutions of functionally graded material Levinson beams, *Acta Mechanica Solida Sinica*, 28, 2015, 592-604.
- [5] Aydogdu, M., Semi-inverse method for vibration and buckling of axially functionally graded beams, *Journal of Reinforced Plastics and Composites*, 27, 2008, 683-691.
- [6] Shahba, A., Attarnejad, R., Marvi, M.T., Free vibration and stability analysis of axially functionally graded tapered


Timoshenko beams with classic and non-classical boundary conditions, *Composites: Part B*, 42, 2011, 801-808.


- [7] Shahba, A., Rajasekaran, S., Free vibration and stability of tapered Euler-Bernoulli beams made of axially functionally graded materials, *Applied Mathematical Modelling*, 36, 2012, 3094-3111.
- [8] Rychlewska, J., Buckling analysis of axially functionally graded beams, *Journal of Applied Mathematics and Computational Mechanics*, 13, 2014, 103-108.
- [9] Torki, M.E., Reddy, J.N., Buckling of functionally-graded beams with partially delaminated piezoelectric layers, *International Journal of Structural Stability and Dynamics*, 16, 2016, 1450104 (25 pages).
- [10] Shvartsman, B., Majak, J., Numerical method for stability analysis of functionally graded beams on elastic foundation, *Applied Mathematical Modelling*, 40, 2016, 3713-3719.
- [11] Huang, Y., Zhang, M., Rong, H.W., Buckling analysis of axially functionally graded and non-uniform beams based on Timoshenko theory, *Acta Mechanica Solida Sinica*, 29, 2016, 200-207.
- [12] Nguyen, T.K., Vo, T.P., Nguyen, B.D., Lee, J., An analytical solution for buckling and vibration analysis of functionally graded sandwich beams using a quasi-3D shear deformation theory, *Composite Structures*, 156, 2016, 238-252.
- [13] Thai, C.H., Ferreira, A.J.M., Abdel Wahab, M., Nguyen-Xuan, H., A moving Kriging meshfree method with naturally stabilized nodal integration for analysis of functionally graded material sandwich plates, *Acta Mechanica*, 229, 2018, 2997-3023.
- [14] Kiani, Y., Eslami, M.R., Thermal buckling analysis of functionally graded materials beams, *International Journal of Mechanics and Materials in Design*, 6, 2010, 229-238.
- [15] Wattanasakulpong, N., Gangadhara Prusty, B., Kelly, D.W., Thermal buckling and elastic vibration of third-order shear deformable functionally graded beams, *International Journal of Mechanical Sciences*, 53, 2011, 734-743.
- [16] Kiani, Y., Taheri, S., Eslami, M.R., Thermal buckling of piezoelectric functionally graded material beams, *Journal of Thermal Stresses*, 34, 2011, 835-850.
- [17] Kiani, Y., Rezaei, M., Taheri, S., Eslami, M.R., Thermo-electrical buckling of piezoelectric functionally graded material Timoshenko beams, *International Journal of Mechanics and Materials in Design*, 7, 2011, 185-197.
- [18] Fallah, A., Aghdam, M.M., Thermo-mechanical buckling and nonlinear free vibration analysis of functionally graded beams on nonlinear elastic foundation, *Composites: Part B*, 43, 2012, 1523-1530.
- [19] Fu, Y., Chen, Y., Zhang, P., Thermal buckling analysis of functionally graded beam with longitudinal crack, *Meccanica*, 48, 2013, 1227-1237.
- [20] Anand Rao, K.S., Gupta, R.K., Ramchandran, P., Rao, G.V., Thermal buckling and free vibration analysis of heated functionally graded material beams, *Defense Science Journal*, 63, 2013, 315-322.
- [21] Kiani, Y., Eslami, M.R., Thermalmechanical buckling of temperature-dependent FGM beams, *Latin American Journal of Solids and Structures*, 10, 2013, 223-245.
- [22] Esfahani, S.E., Kiani, Y., Eslami, M.R., Non-linear thermal stability analysis of temperature dependent FGM beams supported on non-linear hardening elastic foundations, *International Journal of Mechanical Sciences*, 69, 2013, 10-20.
- [23] Ghiasian, S.E., Kiani, Y., Eslami, M.R., Nonlinear thermal dynamic buckling of FGM beams, *European Journal of Mechanics - A/Solids*, 54, 2015, 232-242.
- [24] Sun, Y., Li, S.R., Batra, R.C., Thermal buckling and post-buckling of FGM Timoshenko beams on nonlinear elastic foundation, *Journal of Thermal Stresses*, 39, 2016, 11-26.
- [25] Trinh, L.C., Vo, T.P., Thai, H.T., Nguyen, T.K., An analytical method for the vibration and buckling of functionally graded beams under mechanical and thermal loads, *Composites: Part B*, 100, 2016, 152-163.
- [26] Shen, A.G., Malekzadeh, P., Ziaee, S., Thermoelastic buckling analysis of pre-twisted functionally graded beams with temperature-dependent material properties, *Acta Astronautica*, 133, 2017, 1-13.
- [27] Nguyen, T.K., Nguyen, B.D., Vo, T.P., Thai, H.T., Hygro-thermal effects on vibration and thermal buckling behaviours of functionally graded beams, *Composite Structures*, 176, 2017, 1050-1060.
- [28] Hosseini, M., Farhatnia, F., Oveissi, S. Functionally graded Timoshenko beams with elastically-restrained edge supports: thermal buckling analysis via Stokes' transformation technique, *Research on Engineering Structures & Materials*, 4, 2018, 103-125.
- [29] Majumdar, A., Das, D., A study on thermal buckling load of clamped functionally graded beams under linear and nonlinear thermal gradient across thickness, *Proceedings of the Institution of Mechanical Engineers, Part L: Journal of Materials: Design and Applications*, 232, 2018, 769-784.
- [30] Liu, Y., Su, S., Huang, H., Liang, Y., Thermal-mechanical coupling buckling analysis of porous functionally graded sandwich beams based on physical neutral plane, *Composites: Part B*, 168, 2019, 236-242.
- [31] Thanh, C.L., Tran, L.V., Bui, T.Q., Nguyen, H.X., Abdel-Wahab, M., Isogeometric analysis for size-dependent nonlinear thermal stability of porous FG microplates, *Composite Structures*, 221, 2019, 110838.
- [32] Zhang, J., Chen, L., Lv, Y., Elastoplastic thermal buckling of functionally graded material beams, *Composite Structures*, 224, 2019, 111014.
- [33] Ugural, A.C., *Mechanical Design: An Integrated Approach*, McGraw-Hill Company, Singapore, 2004.
- [34] Chen, W.R., Chang, H., Closed-form solutions for free vibration frequencies of functionally graded Euler-Bernoulli beams, *Mechanics of Composite Materials*, 53, 2017, 79-98.
- [35] Chen, W.R., Chang, H., Vibration analysis of functionally graded Timoshenko beams, *International Journal of Structural Stability and Dynamics*, 18, 2018, 1850007 (24 pages).

- [36] Touloukian, Y.S., *Thermophysical properties of high temperature solids materials*, MacMillan, New York, 1967.
- [37] Reddy, J.N., Chin, C.D., Thermomechanical analysis of functionally graded cylinders and plates, *Journal of Thermal Stresses*, 21, 1998, 593–626.
- [38] Shen, H., *Functionally graded materials, Non-linear analysis of plates and shells*, CRC press, New York, 2009.

ORCID iD

Wei-Ren Chen  <https://orcid.org/0000-0002-4655-8769>

Chun-Sheng Chen  <https://orcid.org/0000-0002-8343-4757>

Heng Chang  <https://orcid.org/0000-0002-9518-4599>



© 2020 by the authors. Licensee SCU, Ahvaz, Iran. This article is an open access article distributed under the terms and conditions of the Creative Commons Attribution-NonCommercial 4.0 International (CC BY-NC 4.0 license) (<http://creativecommons.org/licenses/by-nc/4.0/>).